Los Alamos NATIONAL LABORATORY EST.1943

LA-UR-17-23579 (Accepted Manuscript)

Frustrated magnetism in the spin–chain metal Yb Fe P

Baumbach, Ryan E.
Hamlin, James J.
Janoschek, Marc
Singleton, John
Maple, M. Brian

Provided by the author(s) and the Los Alamos National Laboratory (2017-12-15).

To be published in: Journal of Physics: Condensed Matter

DOI to publisher's version: 10.1088/0953-8984/28/4/046004

Permalink to record: http://permalink.lanl.gov/object/view?what=info:lanl-repo/lareport/LA-UR-17-23579

Disclaimer:
Approved for public release. Los Alamos National Laboratory, an affirmative action/equal opportunity employer, is operated by the Los Alamos National Security, LLC for the National Nuclear Security Administration of the U.S. Department of Energy under contract DE-AC52-06NA25396. Los Alamos National Laboratory strongly supports academic freedom and a researcher's right to publish; as an institution, however, the Laboratory does not endorse the viewpoint of a publication or guarantee its technical correctness.

RESEARCH LIBRARY

Journal of Physics: Condensed Matter

PAPER

Frustrated magnetism in the spin–chain metal $Yb_2Fe_{12}P_7$

To cite this article: R E Baumbach *et al* 2016 *J. Phys.: Condens. Matter* **28** 046004

Manuscript version: Accepted Manuscript

Accepted Manuscript is "the version of the article accepted for publication including all changes made as a result of the peer review process, and which may also include the addition to the article by IOP Publishing of a header, an article ID, a cover sheet and/or an 'Accepted Manuscript' watermark, but excluding any other editing, typesetting or other changes made by IOP Publishing and/or its licensors"

This Accepted Manuscript is © **© 2016 IOP Publishing Ltd**.

During the embargo period (the 12 month period from the publication of the Version of Record of this article), the Accepted Manuscript is fully protected by copyright and cannot be reused or reposted elsewhere.
As the Version of Record of this article is going to be / has been published on a subscription basis, this Accepted Manuscript is available for reuse under a CC BY-NC-ND 3.0 licence after the 12 month embargo period.

After the embargo period, everyone is permitted to use copy and redistribute this article for non-commercial purposes only, provided that they adhere to all the terms of the licence https://creativecommons.org/licences/by-nc-nd/3.0

Although reasonable endeavours have been taken to obtain all necessary permissions from third parties to include their copyrighted content within this article, their full citation and copyright line may not be present in this Accepted Manuscript version. Before using any content from this article, please refer to the Version of Record on IOPscience once published for full citation and copyright details, as permissions will likely be required. All third party content is fully copyright protected, unless specifically stated otherwise in the figure caption in the Version of Record.

View the article online for updates and enhancements.

This content was downloaded from IP address 192.12.184.6 on 15/12/2017 at 18:59

IOPscience

Manuscript version: Accepted Manuscript

The "**Accepted Manuscript**" is the author's original version of an article including any changes made following the peer review process but excluding any editing, typesetting or other changes made by IOP Publishing and/or its licensors.

During the embargo period (the 12 month period from publication of the Version of Record of this article), the Accepted Manuscript:

- is fully protected by copyright and can only be accessed by subscribers to the journal;
- cannot be reused or reposted elsewhere by anyone unless an exception to this policy has been agreed in writing with IOP Publishing

As the Version of Record of this article is going to be/has been published on a subscription basis, this Accepted Manuscript will be available for reuse under a CC BY-NC-ND 3.0 licence after a 12 month embargo period.

After the embargo period, everyone is permitted to copy and redistribute this article for Non-Commercial purposes only, provided they*:

- give appropriate credit and provide the appropriate copyright notice;
- show that this article is published under a CC BY-NC-ND 3.0 licence;
- provide a link to the CC BY-NC-ND 3.0 licence;
- provide a link to the Version of Record;
- do not use this article for commercial advantage or monetary compensation; and
- only use this article in its entirety and do not make derivatives from it.

*Please see CC BY-NC-ND 3.0 licence for full terms.

View the Version of Record for this article online at iopscience.org

This content was downloaded from IOPscience

Classification: Physical Science: Physics

Frustrated magnetism in the spin−chain metal $Yb_2Fe_{12}P_7$

R. E. Baumbach[1],* J. J. Hamlin[1],† M. Janoschek[1],‡ J. Singleton[2], and M. B. Maple[1§]
[1]*Department of Physics, University of California, San Diego, La Jolla, California 92093 and*
[2]*NHMFL, Los Alamos National Laboratory, MS E536,*
Los Alamos, New Mexico 87545, USA

(Dated: October 8, 2015)

Magnetization measurements for magnetic fields $\mu_0 H$ up to 60 T are reported for the noncentrosymmetric spin−chain metal $Yb_2Fe_{12}P_7$. These measurements reveal behavior that is consistent with Ising-like spin chain magnetism that produces pronounced spin degeneracy. In particular, we find that although a Brillouin field dependence is observed in $M(H)$ for $H \perp$ c with a saturation moment that is close to the expected value for free ions of Yb^{3+}, non-Brillouin-like behavior is seen for $H \parallel$ c with an initial saturation moment that is nearly half the free ion value. In addition, hysteretic behavior that extends above the ordering temperature T_M is seen for $H \parallel$ c but not for $H \perp$ c, suggesting out-of-equilibrium physics. This point of view is strengthened by the observation of a spin reconfiguration in the ordered state for $H \parallel$ c which is only seen for $T \leq T_M$ and after polarizing the spins. Together with the heat capacity data, these results suggest that the anomalous low temperature phenomena that were previously reported [R. E. Baumbach et al., *Phys. Rev. Lett.*, **105** 106403 (2010)] are driven by spin degeneracy that is related to the Ising-like one dimensional chain-like configuration of the Yb ions.

I. INTRODUCTION

A significant effort has been made during the past several decades to uncover compounds with exotic phase transitions and unconventional ground states. One such class of materials are transition metal oxides with geometrically frustrated or low dimensional magnetism. In these compounds, the enhanced spin degeneracy at low temperatures drives a variety of unexpected physics.[1,2] A well known example is $SrCu_2(BO_3)_2$, where the spin chain configuration of the Cu ions results in field induced magnetization plateaus at fractional values of the total expected magnetization.[3,4] $Ca_3Co_2O_6$ exhibits similar behavior where the magnetization additionally depends on the field sweep rate, indicating out of equilibrium physics.[5,6] Another group of model frustrated oxides are antiferromagnets on the diamond lattice (e.g., A-site spinel compounds): for instance, $CoAl_2O_4$ exhibits a weak first order phase transition that is limited by kinetic freezing of the domain walls, resulting in glassy behavior.[7] In general, competing magnetic interactions produce the frustration in these compounds: e.g., as for (1) the one-dimensional anisotropic next nearest neighbor Ising (ANNNI) model where different ordered states are nearly degenerate in energy or (2) the three dimensional Ising model with competing interactions.[8–10]

A different route to produce emergent phenomena has been pursued in intermetallic lanthanide and actinide based compounds: most commonly those that include Ce, Yb, U, and Pu.[11–14] A central concept for describing these systems is the competition between the Kondo effect [15] or valence fluctuations [16 and 17], which gradually demagnetize the system as the temperature is reduced through a characteristic Kondo of valence fluctuation temperature, and the RKKY intereaction, which promotes magnetic behavior.[18–20] In the Doniach model, these interactions both depend on the inter-atomic exchange interaction J; when the magnitude of J is finely tuned by varying the chemical composition or applying an external pressure, for example, the opposing interactions can drive a magnetic phase transition to zero temperature at a quantum critical point (QCP).[21] Near the QCP, phenomena including unconventional superconductivity and non-Fermi-liquid (NFL) behavior are often observed.[22,23] A large number of strongly correlated electron compounds have been described in this context: e.g., those with the chemical formulas $CeTIn_5$ (T = Co, Rh, Ir) [24–26] and LnT_2X_2 (Ln = Ce and Yb, T = transition metal, and X = Si and Ge).[27–29]

More recently, it was suggested that magnetic frustration and strong electronic correlations might cooperate to produce ground states that are distinct from those found in frustrated magnets or correlated electron intermetallics.[30–32] An effort to address this subject has been undertaken in several systems that crystallize in the geometrically frustrated Shastry-Sutherland and Kagomé lattices: e.g., as for Yb_2Pt_2Pb [33] and CePdAl [34]. Compounds that crystallize in geometrically non-frustrated lattices (e.g., tetragonal) may also exhibit spin degeneracy due to competing RKKY interactions: e.g., as for the spin spiral phase in $CeRhIn_5$ [35] and competing antiferromagnetic and ferromagnetic phases in $CeRu_2Al_2B$.[36] However, the question of how to tune the frustration and thereby control the related behavior remains unanswered. A clue to solving this problem may be found in correlated electron materials with one dimensional spin chains. In such compounds, the frustration is driven by a delicate balance between n-th nearest neighbor interactions along the chain. Therefore, conventional techniques like applied pressure or chemical substitution

may be adequate to tune the frustration.

Two examples of possible spin chain intermetallics are β-$YbAlB_4$ and $YbNi_4P_2$, which exhibit heavy fermion superconductivity and ferromagnetic quantum criticality, respectively.[37–39] In both of these compounds, the low temperature phenomena are anomalous by comparison to other correlated electron QCP materials, and it has been suggested that these results are related to the chain-like configuration of the Yb ions. However, in both cases, it is not clear that the chains are sufficiently separated spatially to be described as being one-dimensional. Therefore, it remains important to find other correlated electron systems with well separated spin chains. A different family of intermetallic materials which satisfies this criterion are those with the chemical formula $M_2T_{12}Pn_7$ (Fig. 1a,b) where M = Zr, Hf, Ce-Lu, Th, and U, T = Fe, Co, and Ni, and Pn = P and As.[40,41] These compounds exhibit a variety of correlated electron behavior and magnetism including intermediate valence in $Ce_2Fe_{12}P_7$,[42] heavy fermion ferromagnetism in $Sm_2Fe_{12}P_7$,[43] and local moment antiferromagnetism in $U_2Fe_{12}P_7$,[44] making them ideal for investigating the interplay between magnetic frustration and strong electronic correlations.

A particularly interesting example is $Yb_2Fe_{12}P_7$, which has an unusual temperature-magnetic field ($T-H$) phase diagram with an extended region of NFL behavior at low T, as seen in the temperature dependence of the electrical resistivity (Fig. 1c).[45] Additionally, the heat capacity C exhibits an unexpected evolution: C/T increases rapidly below 10 K, exhibits a small peak near the ordering temperature T_M = 0.9 K that is superimposed on a broad hump for $T \leq T_M$ with a maximum value equivalent to a large electronic coefficient of the specific heat $(C/T)_{T=0} = \gamma \approx 3$ J/mol-Yb-K^2 (Fig. 1d), and then displays an additional rapid increase that appears to be the high temperature tail of a nuclear Schottky anomaly. So far, an understanding of the ground state in this system has not been achieved, and it is unclear whether electronic correlations, magnetic frustration, or both are important.

In an effort to obtain further insight into $Yb_2Fe_{12}P_7$, we performed measurements of the magnetization for magnetic fields up to 60 tesla, applied both parallel and perpendicular to the c-axis. This investigation reveals anomalous magnetic behavior where (1) there is no obvious feature in the magnetic susceptibility at the ordering temperature T_M, (2) while a Brillouin field dependence is observed in $M(H)$ for $H \perp$ c with a saturation moment that is close to the expected value for free ions of Yb^{3+}, non-Brillouin-like behavior is seen for $H \parallel$ c with an initial saturation moment that is nearly half the free ion value, (3) hysteretic behavior that extends above T_M is seen for $H \parallel$ c but not $H \perp$ c, suggesting out-of-equilibrium physics when $H \parallel$ c, and (4) a spin reconfiguration occurs in the ordered state for $H \parallel$ c after polarizing the spins, further indicating out-of equilibrium behavior. Together with the heat capacity data, these results suggest that the low temperature phenomena are driven by magnetic frustration that is related to the chain-like arrangement of the Yb ions.

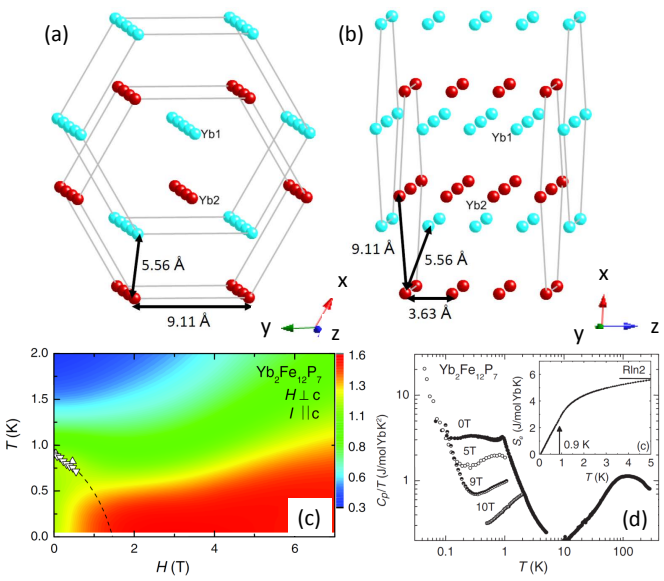

FIG. 1. (a) View of the hexagonal crystal structure of $Yb_2Fe_{12}P_7$ along the c-direction, where the Yb chains are separated by large distances that are filled by Fe and P atoms (not shown). (b) View of the hexagonal crystal structure of $Yb_2Fe_{12}P_7$ along the b direction. (c) Temperature (T) vs. magnetic field (H) phase diagram for $H \perp$ c, reproduced from ref. 45. (d) Heat capacity divided by temperature C/T vs. T, reproduced from ref. 45.

II. EXPERIMENTAL DETAILS

Single crystals of $Yb_2Fe_{12}P_7$ were produced by reacting elements with purities of 99.9% (or better) using a molten Sn flux method.[45] Individual crystals were obtained with a typical needle-like shape. The maximum dimensions were $\sim$ 0.03 cm length and $\sim$ 0.01 cm width.

Isothermal magnetization measurements were performed at the National High Magnetic Field Laboratory at Los Alamos National Laboratory using a 60 T pulsed field magnet and a pumped ^{3}He cryostat. Groups of coaligned single crystals were mounted in grease and were measured using an extraction magnetometer for fields H both perpendicular ($\perp$) and parallel ($\parallel$) to the c-axis.[46] Pulsed magnetic fields were applied with maximum values of $\mu_0 H$ = 2 T, 10 T, and 60 T at constant temperatures 0.4 K $\leq T \leq$ 30 K. The pulsed fields have variable dB/dt over the duration of each shot, with rise times to full field of 20 ms, resulting in maximum shot rates of 550 T/s, 2,800 T/s, and 16,700 T/s for the 2 T, 10 T, and 60 T shots, respectively. Data were collected for both H-rising (red) and H-falling (blue) curves.

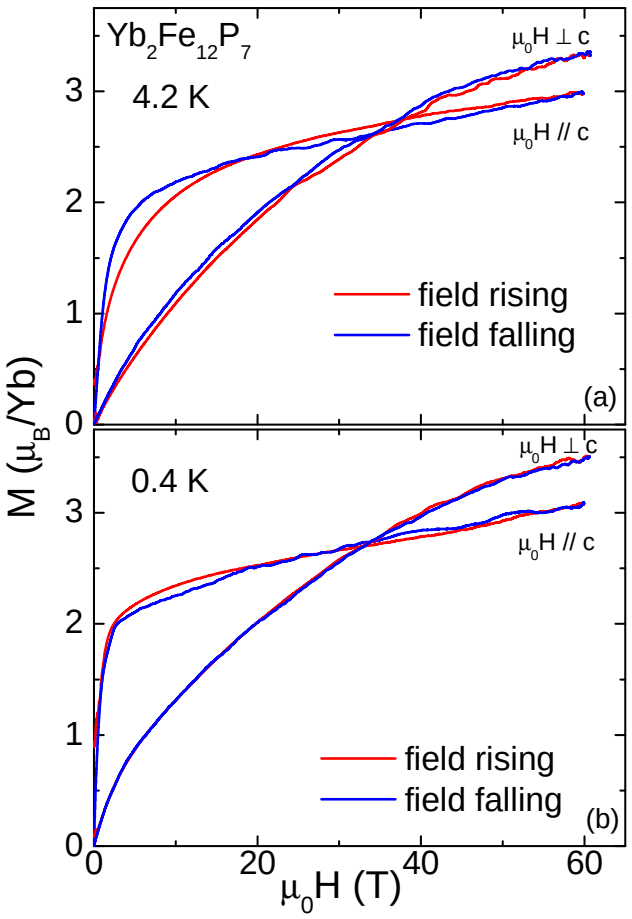

FIG. 2. (a) Magnetization $M_\perp$ and $M_\parallel$ vs field H for H applied perpendicular and parallel to the c-axis at temperature $T = 4.2$ K. The red and blue curves are for rising and falling H, respectively. (b) $M_\perp(H)$ and $M_\parallel(H)$ for $T = 0.4$ K.

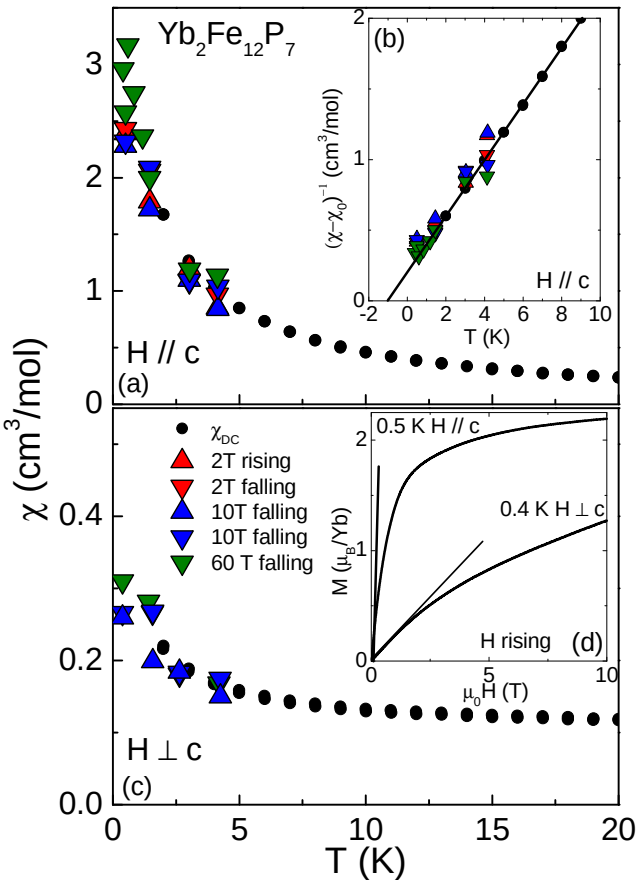

FIG. 3. (a) Magnetic susceptibility $\chi_\parallel$ vs temperature T for fields H applied parallel to the c-axis. (b) Inverse magnetic susceptibility $(\chi_\parallel - \chi_0)^{-1}$ vs T for H applied parallel to the c-axis. (c) Magnetic susceptibility $\chi_\perp(T)$ for H applied perpendicular to the c-axis. (d) Representative $M(H)$ curves. The straight lines yield the initial slopes $(\partial M(H)/\partial H)_{H=0}$ that were used to determine $\chi(T)$, as described in the text.

III. RESULTS

Shown in Fig. 2 are magnetization M versus magnetic field H curves for fields applied both perpendicular and parallel to the c-axis at two representative temperatures, $T = 0.4$ K and 4.2 K. The data were collected up to $\mu_0 H = 60$ T for both field rising (red) and falling (blue). We find pronounced anisotropy in M between the two directions, consistent with our previous measurements which revealed anisotropic magnetism where the c-axis is the easy axis. For both directions, the magnetization approaches $M \approx 3$ - $3.5\mu_B$ at 60 T. For $H \perp$ c ($M_\perp$), almost no hysteresis is observed. In contrast, hysteretic behavior is seen for $H \parallel$ c ($M_\parallel$), where similar hysteresis is also observed in low-field (10 - 20 T) pulses. We will return to the issue of hysteresis below. Here, we also find that the curves cross near 35 T. However, it is not clear that this is an intrinsic effect, since the absolute value of M is obtained by matching the pulsed field data with data that were obtained in a Quantum Design MPMS. As shown in Fig. 3, this procedure leads to uncertainty in the absolute value of M at small H: e.g., for H // c, we find a scatter in $\chi(T = 1.8$ K) ranging from 2.25 - 3 cm^3/mol, which is sufficient to produce the extrinsic crossing in $M(H)$ that is seen at large H.

In order to compare to earlier magnetic susceptibility $\chi(T) = M/H$ measurements, we consider the initial slopes $(\partial M/\partial H)_{H=0}$ of the H-rising and H-falling curves from 2 T, 10 T, and 60 T shots (representative $M(H)$ curves are shown in Fig. 3(d)). From this analysis we find that the values of $(\partial M/\partial H)_{H=0}$ overlap with our previous data (Fig. 3(a,c)). For $H \parallel$ c, $\chi(T)$ exhibits Curie-Weiss (CW) behavior,

$$\chi(T) = \chi_0 + C/(T - \theta) \quad (1)$$

where the effective magnetic moment ($\mu_{\rm eff} = 4.47\ \mu_B$) is close to what is expected for Yb^{3+} free ions ($\mu_{\rm eff} = 4.53\ \mu_B$). As shown in Fig. 3(b), the CW behavior extends to 0.4 K without revealing a clear signature for the

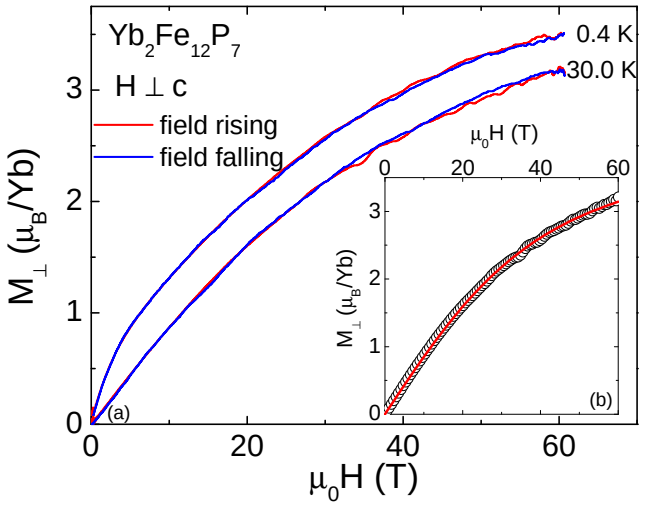

FIG. 4. (a) Magnetization $M_\perp$ vs field H for H applied perpendicular to the c-axis. The red and blue curves are for rising and falling H, respectively. (b) $M_\perp(H)$ for $T = 30$ K. The solid line is a fit to the data using eqn. 2.

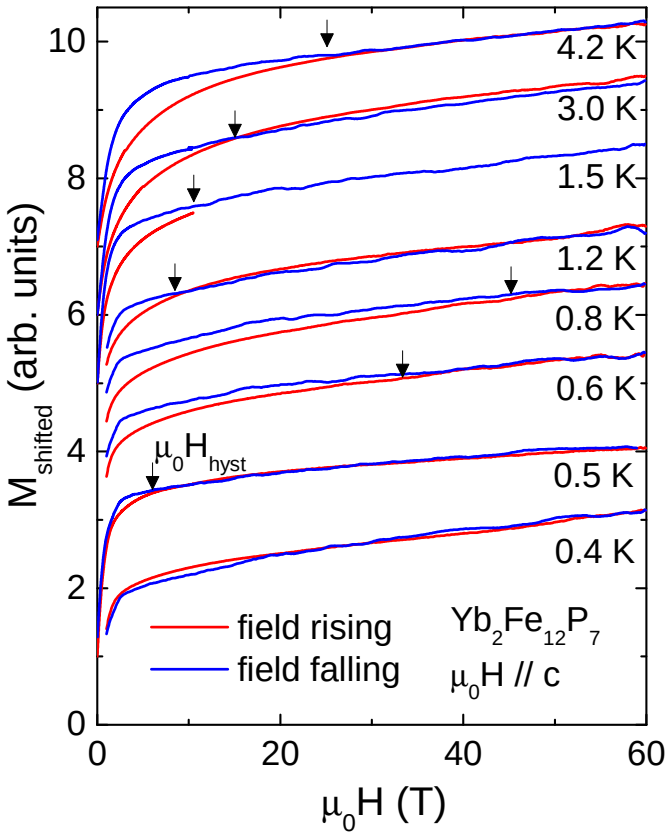

FIG. 5. Magnetization $M_\parallel(H)$ for 60 T shots where the data sets are separated by arbitrary constant offsets to evenly distribute the high field data. The arrows represent H_{hyst}, as defined in the text.

ordering near $T_M = 0.9$ K that was previously seen in electrical resistivity and heat capacity measurements, although the scatter in the data might hide a transition.[45] On the other hand, we might expect that the change in the magnetic susceptibility would be subtle, given that the change in entropy at T_M is small, as shown below. In fact, the small change in entropy may indicate that T_M is a characteristic temperature where partial three dimensional coupling between the chains occurs. We also find that θ = -1 K, which is similar to the ordering temperature T_M. Finally, fits give $\chi_0 = 0.0026$ cm^3/mol. Although this value is somewhat large, it might be attributed to itinerant d-electrons from the Fe ions where $\chi_0 \approx 0.0002$ cm^3/mol-Fe. For $H \perp$ c, $\chi(T)$ continues the low T trend observed previously with no evidence for a phase transition at T_M.

We next consider the $M_\perp(H)$ data in detail (Fig. 4). For $T \geq T_M$, these curves are described by the Brillouin function,

$$M(H) = M_s[\frac{2J+1}{2J}\coth(\frac{2J+1}{2J})y - \frac{1}{2J}\coth(\frac{y}{2J})] \quad (2)$$

where $M_s = Ng_J\mu_B J$ and $y = g_J\mu_B J\mu_0 H/k_B(T-\theta)$, as is expected for a paramagnetic lattice of magnetic moments. From fits to the data (for 4.2 K $\lesssim T \lesssim$ 30 K), we find that $M_s \approx 3.9$ μ_B/Yb. In agreement with previous estimates from Curie-Weiss fits to $\chi(T)$, we also find that $\theta \approx$ -22 K, which suggests that there are antiferromagnetic correlations in the ab plane between the Yb ions. For $T \lesssim 1.4$ K, the initial slope of $M_\perp(H)$ is slightly stronger than expected for a Brillouin function, although these curves are qualitatively similar to those at higher temperatures. As such, it is unclear whether this feature is indicative of magnetic ordering, or instead arises as a result of crystal misalignment with respect to H, which introduces a small fraction of $M_\parallel$ in these measurements.

In contrast to $M_\perp(H)$, the $M_\parallel(H)$ curves show complicated T-H dependences which are non-Brillouin-like (Figs. 2, 5, and 6a,c). For $T \leq T_M$, $M_\parallel(H)$ rises rapidly to values just above 2 μ_B. This behavior is consistent with the small value of θ that was inferred from the CW fit described above. However, instead of approaching a saturation value according to a Brillouin-like field dependence, $M_\parallel(H)$ continues to increase gradually up to 60 T. The falling curve subsequently lags behind the rising curve (except for $T = 0.4$ K, where the hysteresis is due to instability in the measurement) at a characteristic irreversibility field H_{hyst} (arrows in Fig. 5). Comparable hysteresis is not observed when the field is applied perpendicular to c, suggesting that this behavior is intrinsic to the compound and not an experimental artifact. Finally, the falling curves exhibit an additional kink at H_M in the low H region (Fig. 6a). In order to emphasize this feature, we plot $\partial M/\partial H$ (Fig. 6b) where a step-like feature is seen at H_M that moves to lower H with increasing T. We suggest that this feature is related to a spin reorientation phase boundary, but emphasize that it is only

seen for H-falling curves. For $T \geq T_{\rm M}$, the crossover between low/high H is more gradual than is seen for $T \leq T_{\rm M}$, although $M(H)$ remains non-Brillouin-like (Fig. 6c). Again, the rising and falling curves match each other in the high H region and the falling curve lags behind the rising curve for lower H, showing that the irreversibility persists above $T_{\rm M}$. Taken together, these results suggest that for $H \parallel$ c, the spins experience an out of equilibrium condition when they are polarized using a pulsed magnetic field. We further note that similar size hysteresis appears in low-field (2 and 10 T) pulses with slower sweep rates.

In order to show that these features are not due to a magnetocaloric effect, we present the following arguments. First, we note that the full expression for the magnetocaloric effect (i.e., change in temperature, ΔT) on altering the applied magnetic field from H_1 to H_2 under adiabatic conditions is,

$$\Delta T = -\int_{H_1}^{H_2} \left(\frac{\partial M(H,T)}{\partial T}\right)_H \left(\frac{T}{C(H,T)}\right)_H dH \quad (3)$$

where $C(T,H)$ is the heat capacity. We also point out that, by design, a low temperature pulsed-field magnetometry experiment is not adiabatic; the change in field occurs over a timescale of several milliseconds and the sample is surrounded by a cryogenic exchange liquid (^{3}He or ^{4}He), and heat-sunk to the sample holder and silicone grease. Using this setup, we find that (1) the experimentally observed hysteresis in $M(H)$ is of a similar size in low-field (2 - 10 T) pulses as it is in 60 T pulses. All pulses are of the same duration, and therefore the heating rates for low-field and high-field pulses will differ, whereas the available cooling power will remain the same. If the hysteresis were due purely to sample temperature changes, we would expect larger hysteresis for the 60 T shots; this is not the case. (2) Referring to Figs. 3 and 1, $|(\partial M/\partial H)_{H\to 0}|$ seems to increase monotonically in magnitude with decreasing temperature. Between 0.1 and 1 K, C/T is roughly constant in zero field; as the temperature increases further, C/T falls by about a factor of 10 between 1 K and 4.0 K (Fig. 1d). The variation in C/T is smaller at finite field. Over the same temperature range (1 - 4 K), $|(\partial M/\partial H)_{H\to 0}|$ also falls by a factor of 10. Therefore, according to Equation 3, if the magnetocaloric effect were responsible for the hysteresis, we would expect the largest hysteresis at the lowest temperatures. As can be seen from the data, the converse is the case, with the hysteresis almost vanishing at 0.4 K. (3) Comparing the $M(H)$ curves for falling field (blue) and bath temperatures ranging from 0.5 K to 4.2 K in Fig. 5, it can be seen that $M(H)$ has very little temperature dependence above 3 T. Therefore, if the only effect present were a magnetocaloric effect (i.e., a change in temperature), we would expect the $M(H)$ curves on the upsweeps to overlay the M(H) curves on the down sweeps, whereas this is not the case. In conclusion, the magnetocaloric effect can only make a minor contribution to the hysteresis, which must instead be intrinsic to the dynamics of a frustrated magnetic system.

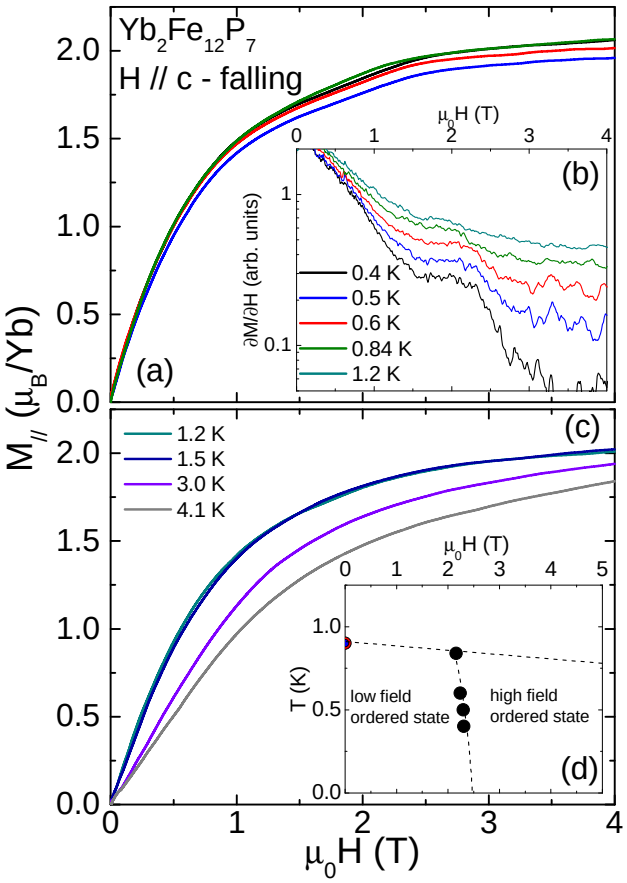

FIG. 6. (a) Magnetization $M_\parallel$ vs field H for H applied parallel to the c-axis for $\mu_0 H \leq 4$ T and $T \leq T_{\rm M} \approx 0.9$ K. (b) $\partial M(H)/\partial H$ for H applied parallel to the c-axis and falling from 60 T. Similar features are observed in the falling curves for 10 T shots. (c) Magnetization $M_\parallel$ vs field H for H applied parallel to the c-axis for $\mu_0 H \leq 4$ T and $T \geq T_M$. (d) $T-H$ phase diagram in the vicinity of the ordered state.

IV. DISCUSSION

The magnetization data reveal behavior that is consistent with strong spin degeneracy at low temperatures. First, we find that the initial saturation moment for $H \parallel$ c is roughly half the expected value for the entire Yb^{3+} Hund's rule multiplet, while larger fields cause $M(H)$ to gradually increase in a non-Brillouin-like manner. This result is in contrast to what is seen when $H \perp$ c, where $M(H)$ follows a typical Brillouin field dependence with $M_s = 3.9$ $\mu_{\rm B}$/Yb, as expected for magnetic Yb^{3+} ions. Although crystalline electric field splitting of the Hund's rule multiplet followed by mixing of the CEF split levels at high fields may be partially responsible for this behavior, it is also possible that it involves

arrested spin polarization that arises from magnetic frustration. Such behavior is seen in the spin chain insulators $SrCu_2(BO_3)_2$ and $Ca_3Co_2O_6$.[3,5] In addition, hysteresis appears in pulsed magnetic fields for $Yb_2Fe_{12}P_7$ when $H \parallel$ c, but not when $H \perp$ c. Since no evidence for ferromagnetism has been seen in this compound, it is likely that this result is due to out of equilibrium spin dynamics that are associated with the Yb spin chains along the c-axis. We also note that the hysteretic behavior extends well above the ordering temperature $T_M \approx 0.9$ K, indicating that spin frustration persists to higher temperatures. Similar behavior is observed for the spin chain compound $Ca_3Co_2O_6$, where pronounced hysteretic behavior extends above the ordering temperature.[3] From these data, we additionally construct a $T - H$ phase diagram for $H \parallel$ c (Fig. 6d). At low T and H, the ordered state is circumscribed by H_M and extends to $\mu_0 H \approx 2.5$ T in the $T = 0$ limit, possibly revealing a quantum phase transition between two distinct spin configurations. However, we emphasize that the kink that defines the putative phase boundary is only seen in the H-falling curves. Further measurements such as neutron scattering or nuclear magnetic resonance are needed to address the issue of whether H_M defines a phase boundary.

To better understand this behavior, we consider the 4f contribution to the heat capacity $C_{4f}(T)$ (Fig. 7a), obtained by subtracting $C(T)$ for the nonmagnetic analogue $Th_2Fe_{12}P_7$ from that of $Yb_2Fe_{12}P_7$. From these data, we see a large hump between 20 - 25 K which can be fitted by an expression of the form,

$$C_{Sch} = R(\frac{\Delta}{T})^2 \frac{\frac{g_0}{g_1} exp\frac{\Delta}{T}}{(1 + \frac{g_0}{g_1} exp\frac{\Delta}{T})^2} \quad (4)$$

(solid line, Fig. 7a) which describes a two-level system. This expression would be a good approximation to the data if the $J = 7/2$ Yb^{3+} multiplet is split by the crystalline electric field (CEF), resulting in CEF split doublets where the lowest energy excited state is well separated from the higher energy excited states. From this expression, we find that $\Delta = 58$ K and $g_0/g_1 = 0.5$, which are the splitting between the ground state and the first excited state and the ratio of the degeneracies of the ground and first excited states, respectively, possibly suggesting that the ground state is a doublet and the first excited state is a quartet.

We next calculate the 4f contribution to the entropy S_{4f} (Fig. 7b) where we find that S_{4f} rises to Rln2 near 10 K (consistent with a doublet ground state), goes through an inflection point, and subsequently goes through another hump near 20 - 25 K due to the CEF splitting. We note that evidence for CEF splitting with an energy scale of $\Delta \approx 50$ K is also observed in our previous measurements of electrical resistivity, magnetic susceptibility, and thermopower.[41,45] Since Rln2 is recovered by 10 K, it appears that the Kondo temperature is rather low ($T_K < 1$ K). If this is true, then it is appropriate to attribute the low temperature behavior to pure localized

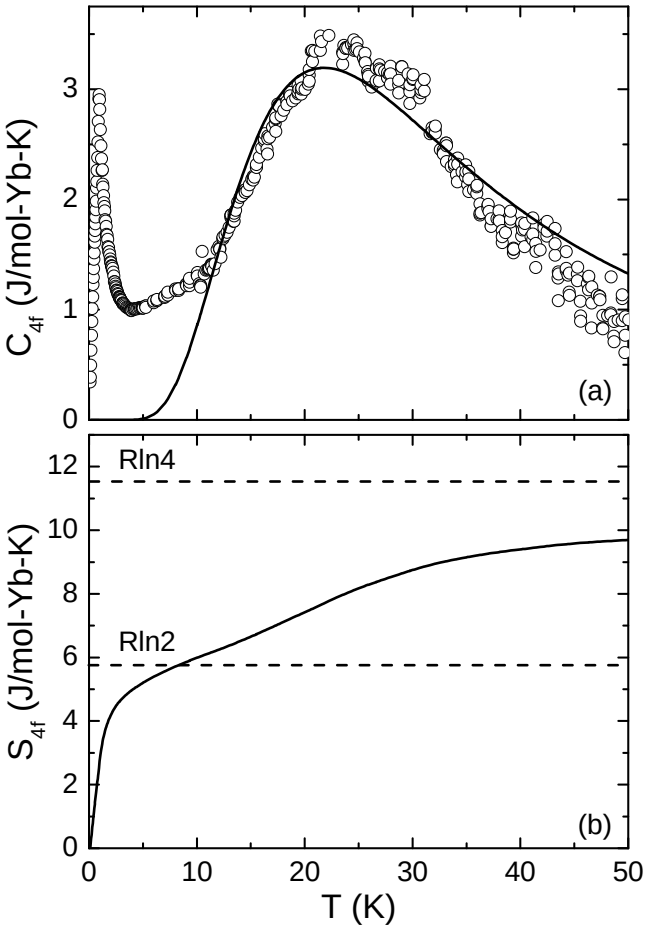

FIG. 7. (a) The 4f contribution to the heat capacity C vs. temperature T for $Yb_2Fe_{12}P_7$, which was obtained as described in the text. The solid line is a two level Schottky fit to the data which arises due to the crystalline electric field splitting of the Yb^{3+} Hund's rule multiplet. (b) The 4f contribution to the entropy S vs. T.

moment physics. This is in contrast to many other Yb-based intermetallics where hybridization of the localized 4f- and conduction electron states in the Yb Kondo lattice is strong enough to produce heavy fermion behavior. Moreover, since the Rln2 of magnetic entropy that is associated with the doublet ground state is only recovered near $10T_M$, it is likely that the frustrated magnetic correlations are present well above T_M, consistent with the observation of hysteretic behavior for $T \geq T_M$.

Finally, we remark that unlike the related insulating spin chain oxides referenced above, $Yb_2Fe_{12}P_7$ is metallic. Therefore, the electronic transport properties are likely to be influenced by the frustrated magnetism. In a previous study, we found that for $H \perp$ c, the electrical resistivity exhibits a non-Fermi-liquid temperature dependence over a large range of magnetic fields and is not obviously associated with a quantum critical point (Fig. 1c).[45] Based on our current result, this behavior

may be related to the spin chain magnetism which couples to the electronic transport properties. This raises the interesting possibility these spin chain metals may be platforms for driving unconventional metallic ground states, as has already been discussed for β-$YbAlB_4$ and $YbNi_4P_2$.[37–39]

V. CONCLUDING REMARKS

We have demonstrated that $Yb_2Fe_{12}P_7$ exhibits a variety of unusual types of magnetic behavior including out of equilibrium magnetism, incomplete spin polarization, a possible spin reconfiguration transition, and buildup of magnetic entropy at low temperatures. Such behavior is unusual in Yb-based metals, where strong electronic correlations that originate from the Kondo effect or valence fluctuations typically dominate the low temperature behavior of the physical properties. However, in the present case, the observed behavior and crystal structure are reminiscent of spin chain oxides. This scenario is particularly attractive because, unlike in insulating spin chain oxides, the magnetism influences the electronic transport behavior and thereby provides a driving mechanism to produce emergent phenomena. For instance, it seems possible that the anomalous non-Fermi-liquid behavior that was previously observed stems directly from the spin chain magnetism. Finally, we note that neutron scattering experiments are essential in order to definitively characterize the magnetic behavior of $Yb_2Fe_{12}P_7$.

VI. ACKNOWLEDGEMENTS

M. Janoschek gratefully acknowledges financial support by the Alexander von Humboldt foundation. We thank J. M. Lawrence and C. D. Batista for stimulating discussions. The structural characterization and physical properties measurements were funded by the United States Department of Energy under research grant DE FG02-04ER46105. Acquisition of crystal growth equipment was funded by the United States Department of Energy under research grant DE FG02-04ER46178.

* Present Address: National High Magnetic Field Laboratory - Florida State University, Tallahassee, Florida 32309, USA

† Present Address: Department of Physics, University of Florida, Gainesville, Florida 32611, USA

‡ Present Address: Condensed Matter and Magnet Science group, Los Alamos National Laboratory, Los Alamos, New Mexico 87545, USA

§ Corresponding Author: mbmaple@ucsd.edu

[1] *Introduction to Frustrated Magnetism: Materials, Experiments, and Theory*, edited by C. Lacroix, P. Mendels, and F. Mila (Springer-Verlag, Berlin, 2011).

[2] *Frustrated Spin Systems*, edited by H. Diep (World Scientific, Singapore, 2004).

[3] H. Kageyama, K. Yoshimura, R. Stern, N. V. Mushnikov, K. Okizuka, M. Kato, K. Kosuge, C. P. Schlichter, and Y. Ueda, *Phys. Rev. Lett.* **82**, 3168 (1999).

[4] S. E. Sebastian, N. Harrison, P. Sengupta, C. D. Batista, S. Francoual, E. Palm, T. Murphy, N. Marcano, H. A. Dabkowska, and B. D. Gaulin, *Proc. Natl. Acad. Sci.* **105**, 20157 (2008).

[5] H. Kageyama, K. Yoshimura, K. Kosuge, H. Mitamura, and T. Goto, *J. Phys. Soc. Jpn.* **66**, 1607 (1997).

[6] V. Hardy, M. R. Lees, O. A. Petrenko, D. McK. Paul, D. Flahaut, S. Hébert, and A. Maignan, *Phys. Rev. B* **70**, 064424 (2004).

[7] G. J. MacDougall, D. Gouta, J. L. Zarestkyd, G. Ehlersa, A. Podlesnyaka, M. A. McGuire, D. Mandrus, and S. E. Nagler, *Proc. Natl. Acad. Sci.* **108**, 15693 (2011).

[8] Y. Kamiya and C. D. Batista, *Phys. Rev. Lett.* **109**, 067204 (2012).

[9] W. Selke and P. M. Duxbury, *Z. Phys. B* **57**, 49 (1984).

[10] P. Bak and J. v. Boehm, *Phys. Rev. B* **21**, 5297 (1980).

[11] G. R. Stewart, *Rev. Mod. Phys.* **73**, 797 (2001).

[12] H. v. Löhneysen, A. Rosch, M. Vojta, and P. Wöfle, *Rev. Mod. Phys.* **79**, 1015 (2007).

[13] C. Pfleiderer, *Rev. Mod. Phys.* **81**, 1551 (2009).

[14] J. L. Sarrao, L. A. Morales, J. D. Thompson, B. L. Scott, G. R. Stewart, F. Wastin, J. Rebizant, P. Boulet, E. Colineau, and G. H. Lander, *Nature* **420**, 297 (2002).

[15] J. Kondo, *Prog. Theor. Phys.* **32**, 37 (1964).

[16] M. R. MacPherson, G. E. Everett, D. Wohlleben, and M. B. Maple, *Phys. Rev. Lett.* **26**, 20 (1971).

[17] M. B. Maple and D. Wohlleben, *Phys. Rev. Lett.* **27**, 511 (1971).

[18] M. A. Ruderman and C. Kittel, *Phys. Rev.* **96**, 99 (1954).

[19] T. Kasuya, *Prog. Theor. Phys.* **16**, 45 (1956).

[20] K. Yosida, *Phys. Rev.* **106**, 893 (1957).

[21] S. Doniach, *Physica B + C* **91**, 231 (1977).

[22] M. B. Maple, R. E. Baumbach, J. J. Hamlin, D. A. Zocco, B. J. Taylor, N. P. Butch, J. R. Jeffries, S. T. Weir, B. C. Sales, D. Mandrus, M. A. McGuire, A. S. Sefat, R. Jin, Y. K. Vohra, J.-H. Chu, and I. R. Fisher *Physica B* **404**, 2924 (2009).

[23] M. B. Maple, R. E. Baumbach, N. P. Butch, J. J. Hamlin, and M. Janoschek, *J. Low Temp. Phys* **161**, 4 (2010).

[24] C. Petrovic, P. G. Pagliuso, M. F. Hundley, R. Movshovich, J. L. Sarrao, J. D. Thompson, Z. Fisk, and P. Monthoux, *J. Phys.: Condens. Mat.* **13**, L337 (2001).

[25] H. Hegger, C. Petrovic, E. G. Moshopoulou, M. F. Hundley, J. L. Sarrao, Z. Fisk, and J. D. Thompson, *Phys. Rev. Lett.* **84**, 4986 (2000).

[26] C. Petrovic, R. Movshovich, M. Jaime, P. G. Pagliuso, M. F. Hundley, J. L. Sarrao, Z. Fisk, and J. D. Thompson, *Europhys. Lett.* **53**, 354 (2001).

[27] R. Movshovich, T. Graf, D. Mandrus, J. D. Thompson, J. L. Smith, and Z. Fisk, *Phys. Rev. B* **53**, 8241 (1996).

[28] H. Q. Yuan, F. M. Grosche, M. Deppe, C. Geibel, G. Sparn, and F. Steglich, *Science* **302**, 2104 (2003).

[29] J. Custers, P. Gegenwart, H. Wilhelm, K. Neumaier, Y. Tokiwa, O. Trovarelli, C. Geibel, F. Steglich, C. Pepin, and P. Coleman, *Nature* **424**, 524 (2003).

[30] P. Coleman and A. H. Nevidomskyy, *J. Low Temp. Phys* **161**, 182 (2010).

[31] C. Lacroix, *J. Phys. Soc. Jpn.* **79**, 011008 (2010).

[32] B. H. Bernhard, B. Coqblin, C. Lacroix, *Phys. Rev. B* **83**, 214427 (2011).

[33] M. S. Kim, M. C. Bennett, and M. C. Aronson, *Phys. Rev. B* **77**, 144425 (2008).

[34] A. Dönni, G. Ehlers, H. Maletta, P. Fischer, H. Kitazawa, and M. Zolliker, *J. Phys.: Condens. Matt.* **8**, 11213 (1996).

[35] T. Park, V. A. Sidorov, F. Ronning, J.-X. Zhu, Y. Tokiwa, H. Lee, E. D. Bauer, R. Movshovich, J. L. Sarrao, J. D. Thompson, *Nature* **456**, 366 (2008).

[36] R. E. Baumbach, H. Chudo, H. Yasuoka, F. Ronning, E. D. Bauer, and J. D. Thompson, *Phys. Rev. B* **85**, 094422 (2012).

[37] S. Nakatsuji, K. Kuga, Y. Machida, T. Tayama, T. Sakakibara, Y. Karaki, H. Ishimoto, S. Yonezawa, Y. Maeno, E. Pearson, G. G. Lonzarich, L. Balicas, H. Lee, and Z. Fisk, *Nat. Phys.* **4**, 603 (2008).

[38] C. Krellner, S. Lausberg, A. Steppke, M. Brando, L. Pedrero, H. Pfau, S. Tencé, H. Rosner, F. Steglich, and C. Geibel, *New J. Phys.* **13**, 103014 (2011).

[39] A. Steppke, R. Küchler, S. Lausberg, E. Lengyel, L. Steinke, R. Borth, T. Lühmann, C. Krellner, M. Nicklas, C. Geibel, F. Steglich, M. Brando, *Science* **339**, 933 (2013).

[40] W. Jeitschko, D. J. Braun, R. H. Ashcraft, R. Marchand, *J. Solid State Chem.* **25**, 309 (1978).

[41] B. D. White, M. Janoschek, N. Kanchanavatee, K. Huang, L. Shu, S. Jang, D. Y. Tütün, J. J. Hamlin, I. K. Lum, R. E. Baumbach, and M. B. Maple , *New Materials for Thermoelectric Applications: Theory and Experiment* NATO Science for Peace and Security Series B (2013).

[42] M. Reehuis and W. Jeitschko, *J. Phys. Chem. Solids* **50**, 563 (1989).

[43] M. Janoschek, R. E. Baumbach, J. J. Hamlin, I. K. Lum, and M. B. Maple, *J. Phys.: Condens. Mat.* **23**, 094221 (2011).

[44] R. E. Baumbach, J. J. Hamlin, M. Janoschek, I. K. Lum, and M. B. Maple, *J. Phys.: Condens. Mat.* **23**, 094222 (2011).

[45] R. E. Baumbach, J. J. Hamlin, L. Shu, D. A. Zocco, J. R. O'Brien, P.-C. Ho, and M. B. Maple, *Phys. Rev. Lett.* **105**, 106403 (2010).

[46] M. A. Goddard, J. Singleton, P. Sengupta, R. D. McDonald, T. Lancaster, S. J. Blundell, F. L. Pratt, S. Cox, N. Harrison, J. L. Manson, H. I. Southerland and J. A. Schlueter, *New J. Phys.* **10**, 083025 (2008).